PHYSICAL REVIEW LETTERS

Number Fluctuations and Energy Dissipation in Sodium Spinor Condensates

Y. Liu,[1,*] E. Gomez,[2] S. E. Maxwell,[1] L. D. Turner,[3] E. Tiesinga,[1] and P. D. Lett[1,†]

[1]*Joint Quantum Institute, University of Maryland and National Institute of Standards and Technology,
Gaithersburg, Maryland 20899, USA*
[2]*Instituto de Física, Universidad Autónoma de San Luis Potosí, San Luis Potosí 78290, Mexico*
[3]*School of Physics, Monash University, Victoria 3800, Australia*

We characterize fluctuations in atom number and spin populations in $F = 1$ sodium spinor condensates. We find that the fluctuations enable a quantitative measure of energy dissipation in the condensate. The time evolution of the population fluctuations shows a maximum. We interpret this as evidence of a dissipation-driven separatrix crossing in phase space. For a given initial state, the critical time to the separatrix crossing is found to depend exponentially on the magnetic field and linearly on condensate density. This crossing is confirmed by tracking the energy of the spinor condensate as well as by Faraday rotation spectroscopy. We also introduce a phenomenological model that describes the observed dissipation with a single coefficient.

The transition from a thermal atomic gas to a Bose-Einstein condensate (BEC) is marked by the appearance of a scalar order parameter. Spinor BECs have an additional spin degree of freedom which results in a vector order parameter. The increase in complexity leads to the formation of spin domains [1–3], the appearance of novel phases [4] and the possibility of high spatial resolution magnetometry [5]. Spin-1 spinor BECs have been studied with ^{23}Na atoms that show antiferromagnetic interactions [3,6–8] and with ^{87}Rb atoms that show ferromagnetic interactions [2,9–13]. A remarkable result is the observation of spin population oscillations that appear when the system is taken out of equilibrium in the presence of a magnetic field [2,7]. An interplay between the quadratic Zeeman energy and a spin-dependent interaction energy determines the oscillation frequency. The oscillations are nearly harmonic except near a separatrix in phase space where the period diverges [7,8,10]. The system can be forced onto either the low or high energy side of the separatrix using the magnetic field strength [7,10], the BEC density [2], or the balance among spin states [8].

Quantum optical effects in spinor BECs are now being actively studied. Recent experiments observed the spin-mixing analogue of parametric amplification [14]. Number fluctuations and spin oscillations were investigated in a ferromagnetic Rb BEC in Refs. [9,15]. The observed spin oscillations damped and the system reached a steady state, while the fluctuations saturated. Nondissipative theories of quantum effects in number fluctuations [15–18] show that such damped spin oscillations can be produced by dephasing from quantum fluctuations or from number and phase fluctuations in the initial state.

We report observations of the dynamics of atom number fluctuations in an antiferromagnetic ^{23}Na spinor BEC which show strong evidence of energy dissipation. Atom

number fluctuations of the spin projections are extracted from a series of measurements on condensates which spin mix while slowly evolving to the ground state. Because of the dissipation, a spinor BEC with given initial conditions and sufficiently high energy will cross the separatrix at a critical time, t_c. The time evolution of the population fluctuations unambiguously identifies t_c. We have developed a dissipation model that includes a single phenomenological coefficient, is classical, and does not require the intrinsic quantum fluctuations that have been used to describe ferromagnetic Rb spinor systems. Other dissipation mechanisms have been suggested in [12,19,20], but do not explain our data. Mean-field simulations at zero magnetic field including finite temperature effects in Ref. [21] indicate that thermal excitations play a prominent role in the dissipation.

We show that a nondissipative quantum model does not account for our data. This model predicts a damped spin oscillation due to quantum dephasing similar to the ferromagnetic case. Its predicted steady states, however, are very different from the experimental observations in this Letter and Ref. [8]. It is interesting to note that a spinor BEC represents a nominally isolated quantum system that shows dissipation and does not display quantum rephasing over our observation times.

The setup is similar to that of our previous work [8]. We create a $F = 1$ spinor BEC of $N = 1.50(3) \times 10^5$ ^{23}Na atoms through 6 s forced evaporation in a crossed optical dipole trap using a multimode fiber laser at 1070 nm (all quoted uncertainties are 1 standard deviation, combined statistical and systematic). We apply a weak magnetic field gradient during the evaporation to fully polarize the atoms to the $|F = 1, m_F = +1\rangle$ state. The final trap oscillation frequencies are $\omega_0(\sqrt{2}, 1, 1)$ in the three spatial directions. We have performed experiments with measured values of

$\omega_0/(2\pi) = 154(5)$ Hz, $220(7)$ Hz, and $305(9)$ Hz. This corresponds to mean Thomas-Fermi radii of 6 to 8 μm. The density of the BEC is changed only by changing the trap frequency and not by reducing the atom number, as this causes a large loss in signal.

To prepare the initial state, we turn off the magnetic field gradient and ramp to a magnetic field, B, less than 61 μT. We apply an rf pulse resonant with the linear Zeeman splitting (frequencies of hundreds of kHz) to rotate the atomic spin. All of our experiments start with the same initial atomic state which has $\rho_{+1} = \rho_{-1} = 1/4$ and $\rho_0 = 1/2$, where the ρ_{m_F} are fractional populations for the three Zeeman sublevels ($m_F = 0, \pm 1$). This state has zero magnetization, where the magnetization is defined as $m = \rho_{+1} - \rho_{-1}$. We use two methods to detect spin-mixing dynamics: Faraday rotation spectroscopy and Stern-Gerlach separation combined with absorption imaging (SG-AI). Faraday rotation spectroscopy can be used for continuous observation of spin oscillations of a single BEC over short time scales, while SG-AI can directly measure spin populations, albeit destructively [8].

The Mandel Q parameter is a common way to quantify fluctuations in quantum systems, with $Q > 0(<0)$ representing super- (sub-) Poissonian distributions [22]. We use a modified Q parameter to characterize population fluctuations during spin mixing. This Q parameter of ρ_0 is defined as [15]

$$Q = \langle N \rangle \frac{\langle \triangle \rho_0^2 \rangle}{\langle \rho_0 \rangle} - 1, \tag{1}$$

where $\langle N \rangle$ is the mean value of the atom number in the BEC. $\langle \triangle \rho_0^2 \rangle$ and $\langle \rho_0 \rangle$ correspond to the variance and the mean value of ρ_0, respectively. At each delay time after initialization, we extract the variance from 25–30 repeated SG-AI measurements. We use ρ_0 rather than the population, because measurements of ρ_0 and m are less sensitive to the 2% fluctuations in the initial N.

Theoretically, our initial state, prepared from a single component BEC, should be a coherent state with a Poissonian atom number distribution ($Q = 0$). The observed Q at $t = 0$ is equal to 4, while the minimum observable Q at other times depends on the populations, due to technical noise in atom counting. In particular, when one of the spin populations is close to zero the minimum value of, and the error in, Q are larger.

Figure 1 shows the time evolution of Q for $m = 0$ at four magnetic field strengths. Q has a value equal to the experimental limit at $t = 0$, increases to a peak at t_c, then decreases back to the experimental limit within 10 s. We find that at $t = 10$ s all the remaining atoms are in the $m_F = 0$ state ($\approx 20\%$ are lost). A Gaussian fit to $Q(t)$ is applied to extract t_c. We observe that the value of t_c decreases with increasing field. For high fields (e.g., $B = 60.7$ μT in Fig. 1) where the system is on the low energy side of the separatrix at $t = 0$, $Q(t)$ stays at the experimental limit during the whole evolution.
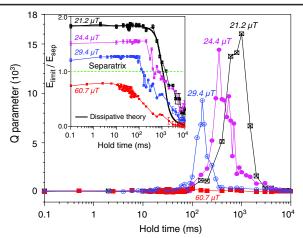

FIG. 1 (color online). Time evolution of Q with $\langle n \rangle = 1.37(6) \times 10^{14}$ cm^{-3} [$c/h = 33(1)$ Hz] at four magnetic fields as indicated in the figure. Inset: Time evolution of $E_{\text{limit}}/E_{\text{sep}}$ for the same data (see text). Good agreement between the predictions of Eqs. (3) and the data is found using a β that falls on the line shown in the inset of Fig. 3. An example curve is shown for $B = 21.2$ μT (thick black line).

The single mode approximation (SMA) [10] appears to be a suitable model to explain our data. In this approximation all the spin components share the same spatial wave function $\Phi(\mathbf{r})$ and the total wave function is $\Psi(\mathbf{r}, t) = \Phi(\mathbf{r})(\sqrt{\rho_{-1}(t)}e^{i\theta_{-1}(t)}, \sqrt{\rho_0(t)}e^{i\theta_0(t)}, \sqrt{\rho_{+1}(t)}e^{i\theta_{+1}(t)})$, where θ_{m_F} represents the phase of each spin component. Taking into account the conservation of m and N, the description simplifies into a model with only two dynamical variables ρ_0 and θ, where $\theta = \theta_{-1} + \theta_{+1} - 2\theta_0$. The classical spinor energy is [10]

$$E = E_{\text{qz}}(1 - \rho_0) + c\rho_0((1 - \rho_0)$$
$$+ \sqrt{(1 - \rho_0)^2 - m^2} \cos\theta), \tag{2}$$

where $E_{\text{qz}} \propto B^2$ is the quadratic Zeeman shift [$E_{\text{qz}}/h = (0.0277 \text{ Hz}/(\mu\text{T})^2)B^2$], $c = c_2\langle n \rangle$ is the spin-dependent interaction energy with the mean BEC density $\langle n \rangle$, and $c_2/h = 2.4 \times 10^{-13}$ Hz cm^3 for ^{23}Na (h is the Planck constant) [7]. In the Thomas-Fermi approximation, $\langle n \rangle$ and c are proportional to $N^{2/5}\omega_0^{6/5}$. The separatrix is the contour in (ρ_0, θ) phase space with energy E_{sep}, on which there is a saddle point where $\dot{\rho}_0 = \dot{\theta} = 0$. For an antiferromagnetic spinor BEC with $m = 0$, $E_{\text{sep}} = E_{\text{qz}}$. The mean-field ground state is $\rho_0 = 1$ for $m = 0$ [8].

The energy of the system cannot be directly inferred from SG-AI measurements. We can, however, use the values of ρ_0 and m to calculate an upper bound (E_{limit}) to the classical spinor energy. In fact, E_{limit} is equal to $(1 - \rho_0^{\text{max}})(E_{\text{qz}} + 2c\rho_0^{\text{max}})$ for $m = 0$, where ρ_0^{max} is the maximum value of ρ_0 among the 25–30 repeated measurements. The inset of Fig. 1 shows that E_{limit} decreases over time and crosses the separatrix around t_c at low fields. This indicates that E is not conserved.

One source of dissipation is loss of BEC atoms and the corresponding decrease in density, resulting in a decrease in c. The interaction energy evolves as $c(t) \propto e^{-2\gamma t/5}$ as follows from the Thomas-Fermi approximation, with $\gamma \leq 0.02$ s^{-1} estimated from the observed atom loss. Because all observed t_c are much smaller than $1/\gamma$, the evolution of c does not explain our data and, hence, is ignored.

In Fig. 2 the evolution of Q is compared to several theoretical models. The dashed line is a result of a non-dissipative quantum simulation based on a quantized version of Eq. (2) following the prescription in Ref. [15]. An initial Gaussian wave packet with a standard deviation in ρ_0 of 0.8% mimics the fluctuations in initial population. A classical Monte Carlo simulation based on Eq. (2) provides a similar result (not shown). We average over 30 trajectories using a Gaussian probability distribution for the same variance of ρ_0. These two nondissipative simulations approach an identical steady-state value of Q; however, they do not explain the observed Q. Moreover, the steady-state spin populations of these models are different from experimental observations.

We modify the equations of motion for ρ_0 and θ [10] by adding a dissipation term inspired by the description of Ohmic loss in Josephson junctions [23]. This leads to

$$\dot{\rho}_0 = -(2/\hbar)\partial E/\partial\theta, \qquad \dot{\theta} = +(2/\hbar)\partial E/\partial\rho_0 + \beta\dot{\rho}_0,$$
(3)

which corresponds to an evolution of the energy given by $dE/dt = -\hbar\beta(\dot{\rho}_0)^2/2$. The solid line in Fig. 2 represents a
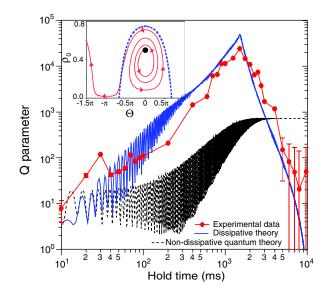

FIG. 2 (color online). Time evolution of Q with $\langle n \rangle = 2.02(8) \times 10^{14}$ cm^{-3} [$c/h = 48(2)$ Hz] at $B = 21.2(1)$ μT. Red (or gray) dots represent experimental data. The dashed (black) line is the result of the nondissipative quantum simulation. The solid (blue or dark gray) line represents a classical Monte Carlo simulation using Eqs. (3) with $\beta \neq 0$. Inset: A classical simulated path including energy dissipation through phase space. The black dot represents the initial state. The (blue) dashed line is the contour with energy E_{sep}.

classical Monte Carlo simulation with this dissipation mechanism. We sample two Gaussian distributions with standard deviations of 0.8% and 1% for the initial values of ρ_0 and c, respectively. The deviation in c is due to the 2% uncertainty in N, while the drift in ω_0 over these measurements is negligible.

By assuming $E(t_c) = E_{sep}$ the coefficient β is obtained, where t_c is the observed critical time. For an extracted β, we find agreement between the observed E_{limit} and the energy derived from the dissipative model, as shown in the inset of Fig. 1. Additionally, including the initial fluctuations enables our model to reproduce the behavior of $Q(t)$ in Fig. 2. The predicted Q, however, is almost twice as large as the experimental value at t_c. Several other phenomenological dissipation terms were tested, but the term $\beta\dot{\rho}_0$ is the only one linear in ρ_0, θ, $\dot{\rho}_0$, or $\dot{\theta}$ that we found to drive the system to the correct ground state [8].

We can understand the evolution of Q from considering the trajectory in the inset of Fig. 2. It shows a simulated path through phase space based on Eqs. (3). The dissipation leads to a gradual decrease of energy, which results in a larger oscillation amplitude in ρ_0 as the trajectory approaches the separatrix. Paths starting from slightly different initial conditions separate after several oscillations. Larger oscillation amplitudes in ρ_0 in these separated paths lead to a larger variance and thus an increasing Q. As the energy decreases past the separatrix, the oscillation amplitude decreases until it goes to zero at the ground state. This reduces Q back to a minimum. Thus Q reaches a maximum as the ensemble crosses the separatrix at time t_c. The energy dissipation is deterministic and does not explain the observed Q by itself. The evolution of Q is a consequence of dephasing due to the spread of initial conditions and the change in oscillation amplitude during the evolution of the system.

Figure 3 shows the measured t_c as a function of B for three densities (and thus for three values of c). The solid lines show exponential fits to the data. Uncertainties are larger for data at the smallest density because we find that $Q(t)$ shows a broader and asymmetric peak and thus it is hard to extract t_c from a single Gaussian fit to $Q(t)$.

The inset of Fig. 3 shows β determined from Eqs. (3) as a function of E_{qz}/c. The coefficient β fits to a linear function with a (dimensionless) slope of 0.22(1). The relation holds for different B and $\langle n \rangle$; hence, a single function seems to describe all the data in terms of a single parameter E_{qz}/c. It is important to note that this same ratio completely determines the shape of the energy surface in phase space for a given m. For very small fields, the fit extrapolates to an unphysical negative β. This indicates that either the dissipation term or the functional form of β are perhaps incomplete or not appropriate. For example, our analysis does not include the coupling of the single BEC mode to other degrees of freedom, such as elementary excitations (whose energies are on the order of $\hbar\omega_0$), which are indicated to be important by Ref. [21].
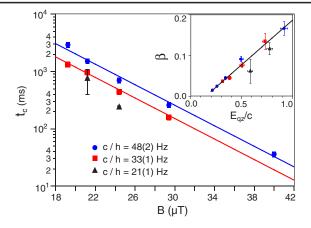
FIG. 3 (color online).   Measured t_c as a function of B at mean densities, $2.02(8) \times 10^{14}$ cm^{-3} (blue or dark gray circles), $1.37(6) \times 10^{14}$ cm^{-3} (red or gray squares), and $0.89(4) \times 10^{14}$ cm^{-3} (black triangles). The solid lines are exponential fits. Inset: β as a function of E_{qz}/c for the same data. The solid line is a weighted linear fit to the data. At the separatrix $E_{qz}/c = 1$.

We have also studied the phase-space dynamics using Faraday rotation spectroscopy. This method can reveal evidence of the separatrix crossing from a single BEC realization. As outlined in Ref. [8], a BEC on the high energy side of the separatrix produces an oscillating Faraday signal with nonzero minima, while on the low energy side the Faraday signal reaches zero. Figure 4 shows an example of the Faraday signal from a single BEC at $B = 36.3(1)$ μT and $m = 0$. The trace shows a transition from nonzero minima to minima near zero, thus providing a clear signature of crossing the separatrix in phase space between 35 and 45 ms. While the details of repeated traces vary, the system always crosses the separatrix during this narrow time interval.
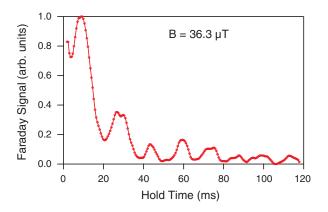

FIG. 4 (color online).   Faraday signal for a single evolving BEC with $\langle n \rangle = 1.37(6) \times 10^{14}$ cm^{-3} $[c/h = 33(1)$ Hz$]$. For this specific case, the initial ρ_0 is 0.45. The transition from the oscillating phase solution to the running phase solution happens between 35 and 45 ms, as shown by the signal periodically approaching zero at the minima afterwards. This is in good agreement with the predicted t_c from Fig. 3.

Figure 4 confirms our assumption that t_c corresponds to a crossing of the separatrix, and t_c from the Faraday signal agrees with the extrapolated value of t_c from Fig. 3. Light-induced atom loss limits our Faraday detection to 100 ms, making it hard to observe the separatrix crossing using Faraday detection for smaller values of B.

In Fig. 4 the rapid reduction of the oscillation amplitude with time is due to atom losses generated by the Faraday beam and not, as might be expected, to energy dissipation. The Faraday beam gradually destroys the spin dynamics by off-resonant light scattering and tensor light-shift dephasing, and thus the Faraday detection is only effective over short observation times.

In conclusion, we have studied spin population fluctuations and energy dissipation in a spinor BEC. Population fluctuations peak at a critical time where the energy of the system equals that of the separatrix in phase space and we have confirmed the separatrix crossing using Faraday rotation spectroscopy. We present a dissipation model with a single phenomenological coefficient that describes our data. While the underlying physics requires further study, this work sheds new light on dissipation mechanisms in a nominally isolated spinor BEC.

*yingmei.liu@nist.gov
†paul.lett@nist.gov
[1] W. Zhang *et al.*, Phys. Rev. Lett. **95**, 180403 (2005).
[2] M. S. Chang *et al.*, Nature Phys. **1**, 111 (2005).
[3] J. Stenger *et al.*, Nature (London) **396**, 345 (1998).
[4] R. Barnett, A. Turner, and E. Demler, Phys. Rev. Lett. **97**, 180412 (2006).
[5] M. Vengalattore *et al.*, Phys. Rev. Lett. **98**, 200801 (2007).
[6] H. J. Miesner *et al.*, Phys. Rev. Lett. **82**, 2228 (1999).
[7] A. T. Black *et al.*, Phys. Rev. Lett. **99**, 070403 (2007).
[8] Y. Liu *et al.*, Phys. Rev. Lett. **102**, 125301 (2009).
[9] M. S. Chang *et al.*, Phys. Rev. Lett. **92**, 140403 (2004).
[10] W. Zhang *et al.*, Phys. Rev. A **72**, 013602 (2005).
[11] J. Kronjager *et al.*, Phys. Rev. Lett. **97**, 110404 (2006).
[12] A. Widera *et al.*, New J. Phys. **8**, 152 (2006).
[13] F. Gerbier *et al.*, Phys. Rev. A **73**, 041602(R) (2006).
[14] C. Klempt, arXiv:0902.2058v1.
[15] L. Chang *et al.*, Phys. Rev. Lett. **99**, 080402 (2007).
[16] C. K. Law, H. Pu, and N. P. Bigelow, Phys. Rev. Lett. **81**, 5257 (1998).
[17] H. Pu *et al.*, Phys. Rev. A **60**, 1463 (1999).
[18] R. B. Diener and T.-L. Ho, arXiv:0608732v1.
[19] M. Erhard *et al.*, Phys. Rev. A **70**, 031602(R) (2004).
[20] H. Schmaljohann *et al.*, Appl. Phys. B **79**, 1001 (2004).
[21] M. Moreno-Cardoner *et al.*, Phys. Rev. Lett. **99**, 020404 (2007).
[22] H. Paul, Rev. Mod. Phys. **54**, 1061 (1982).
[23] S. Kohler and F. Sols, New J. Phys. **5**, 94 (2003).